Thomas K. F. Foo, PhD • Matt A. Bernstein, PhD • Alex M. Aisen, MD[2]
Ramiro J. Hernandez, MD • Bruce D. Collick, PhD • Tsur Bernstein, PhD

Improved Ejection Fraction and Flow Velocity Estimates with Use of View Sharing and Uniform Repetition Time Excitation with Fast Cardiac Techniques[1]

PURPOSE: **To improve the accuracy of ventricular volume estimates and effective temporal resolution in fast cardiac acquisitions.**

MATERIALS AND METHODS: **Data sets at intermediate temporal phases were generated by means of sharing of views from two temporally adjacent data sets. A simulated model was used, and studies with patients and volunteers were conducted. View sharing was implemented in both fast gradient-echo and fast phase-contrast cine acquisitions; breath holding was used when possible.**

RESULTS: **Uniform repetition time (TR) radio-frequency (RF) excitation allowed a better assessment of the end-diastolic ventricular volume. In addition, view sharing provided a better estimate of end-systolic ventricular volume in cases in which rapid changes in volume occurred at or about the temporal boundary of the source images. View sharing also provided a much smoother representation of dynamic cardiac motion when viewed in a cine loop.**

CONCLUSION: **View sharing and uniform TR RF excitation improve the accuracy of end-systolic and end-diastolic ventricular volume measurements by improving the effective temporal resolution.**

Index terms: Heart, volume, 51.92 • Magnetic resonance (MR), phase imaging, 51.12144 • Magnetic resonance (MR), rapid imaging, 51.121416 • Magnetic resonance (MR), volume measurement

Radiology 1995; 195:471–478

In segmented k-space fast cardiac imaging, several groups of multiple k-space lines or views are acquired per cardiac RR interval (1). Each group of n views (number of k-space views per segment) acquired in this manner constitutes a data segment that contributes to the formation of an image at a specific phase of the cardiac cycle. Multiple segments in an RR interval are thus acquired, corresponding to different time points (phases) in the cardiac cycle. A segmented k-space cardiac cine data set with multiple temporal phases of the cardiac cycle can be acquired in a considerably shorter time than conventional gradient-echo cine acquisitions (2); this shorter time makes breath-hold imaging of the cardiovasculature possible. The maximum number of cardiac phases in such a fast acquisition is limited, however, to the number of segments that will fit in an RR interval. The maximum number of phases is then a function of the number of views per segment, the pulse-sequence repetition time (TR), and the patient's heart rate.

In segmented k-space acquisitions, motion is averaged for the period of the segment (or time required to acquire data) for each image; this value is represented as $n \times TR$ in each RR interval. Segments that correspond to different temporal phases of the cardiac cycle are acquired during multiple heartbeats at the same relative delay from the electrocardiogram (ECG) R-wave trigger. If periodic motion, such as that of the heart, is imaged over several RR intervals, with each group of k-space views for a particular image acquired during a segment period, the motion for each image is then the average over the segment period.

We define the effective temporal resolution of an acquisition as the time interval between each reconstructed temporal-phase image. The true temporal resolution of an acquisition is then the result of motion averaged for the segment period. As long as the acquisition or segment period remains unchanged, the true temporal resolution also remains unchanged. We believe that visualization can be improved by increasing the effective temporal resolution even if the true temporal resolution remains unchanged, provided that the motion for each image is averaged for a different instant of time. In this study, we draw a distinction between effective temporal resolution and true temporal resolution.

There are several ways to improve the temporal resolution and thus improve estimation accuracy of the end-systolic state. The first is to improve the true temporal resolution by means of a reduction in the sequence TR. Minimum TRs in the range of 4–6 msec can easily be attained but only with magnetic resonance (MR) imaging devices that have enhanced, high-speed gradient subsystems. An alternative method in systems with conventional gradients (10 mT/m amplitude, 17 T/m/sec slew rate) is to delay the acquisition such that the end-systolic state occurs in the middle of an acquisition segment. It is difficult, however, to determine when this occurs in the cardiac cycle, so this is not a practical solution. Moreover, by delaying the start of the acquisition, the end-diastolic state immediately after the R-wave trigger may be

[1] From the Applied Science Laboratory (T.K.F.F., M.A.B.), Computer Engineering (B.D.C.), and Advanced Applications (T.B.), GE Medical Systems, 3200 N Grandview Blvd, W-875, Waukesha, WI 53188; and the Department of Radiology, University of Michigan, Ann Arbor (A.M.A., R.J.H.). Received June 29, 1994; revision requested August 24; revision received January 10, 1995; accepted January 23. **Address reprint requests to** T.K.F.F.

[2] Current address: Department of Radiology, Indiana University Medical Center, Indianapolis.

Abbreviations: ECG = electrocardiogram, EF = ejection fraction, PC = phase contrast, RF = radio frequency, TR = repetition time, VENC = velocity encoding.

missed. A better solution is to use two acquisitions; the second acquisition should have a delay from the R-wave trigger such that the acquisition period of the data segments in the second acquisition overlaps that of the first by 50%. Images from these two acquisitions can then be combined to provide images at twice the effective temporal resolution. A two-acquisition scheme (double the acquisition time) is time-consuming, however, and results in misregistration due to the separate breath holds. The true temporal resolution is unchanged, but the effective temporal resolution is doubled.

Herein, we present a reconstruction technique that doubles the effective temporal resolution in cine fast cardiac (FASTCARD; GE Medical Systems, Milwaukee, Wis) imaging without an increase in acquisition time. All data are acquired in a single breath hold (if desired) in the usual manner, and data collection is begun immediately after the ECG R-wave trigger. The shifting of the temporal segments in time is achieved by means of sharing of k-space views between two adjacent temporal-phase images to generate an intermediate temporal-phase image. The percentage of views shared determines the implicit delay time of the intermediate segments from the ECG R-wave trigger. In this manner, a single acquisition may yield several more temporal phases by means of sharing of different proportions of data from the original temporally adjacent data sets. We believe this technique improves the effective temporal resolution, but the motion-averaged (true) temporal resolution remains unchanged.

This technique is similar to the MR fluoroscopy method proposed by Riederer et al (3) except that data are acquired during multiple RR intervals and are shared only between segments in the same RR interval. Early results of view sharing were discussed by Laub (4) and Foo et al (5). We discuss view sharing in greater detail and report the results of extension of view sharing to a fast cardiac segmented k-space phase-contrast (PC) cine acquisition (6). Fast cardiac PC with view sharing allows improved temporal resolution in the acquisition of velocity-encoded (VENC) data. This allows flow quantification as a function of delay in the cardiac cycle to be completed within a breath hold.

Better visualization of the end-diastolic state is achieved when data acquisition is begun immediately after the ECG R wave. In the method of Atkinson and Edelman (1), the sequence is prospectively gated. That is, there is some dead time after the last view has been acquired, and data acquisition resumes only after the detection of a valid cardiac trigger. Because of the need to establish a steady state before data acquisition, several dummy radio-frequency (RF) excitations are played out immediately after the cardiac trigger has been detected. This results in a "blind spot" during the end-diastolic phase when no data are being acquired. The end-diastolic cardiac state can be better visualized if data acquisition is begun immediately after detection of the ECG R-wave trigger. One way to accomplish this is to eliminate the dummy RF excitations used to attain a steady state. This elimination is feasible only if the spins are maintained in dynamic equilibrium throughout image acquisition. Dynamic equilibrium can be maintained by means of the uniform application of RF excitation pulses during imaging, even during the time when there is a pause in data acquisition before the next ECG trigger (the "trigger window").

One motivation for our exploration of the proposed technique was the need to develop methods that allow better visualization of the end-diastolic and end-systolic state. Because motion is averaged for a segment period, the end-systolic state may not be accurately depicted. This is especially true when the end-systolic state or rapid volume changes occur at or near the temporal boundary between two adjacent acquisition segments. As the end-systolic state may persist for as little as 40–50 msec, fast segmented k-space cine imaging with a segment period of 80 msec (n = eight views per segment with a TR of 10 msec) may result in an overestimation of the end-systolic ventricular volume. If the end-systolic state occurs in the middle of a temporal segment, then the non–view-shared image provides a more accurate measure of the ventricular volume. Errors in measurement of the maximum and minimum ventricular volumes will result in inaccuracies in the determination of cardiac functional parameters, such as stroke volume and ejection fraction (EF).

In the study by Sakuma et al (7), both left ventricular end-systolic and end-diastolic volumes obtained with fast cardiac imaging had been underestimated when they were compared with values obtained by means of conventional cine MR imaging. A possible explanation is that the true end-diastolic state occurred in their study during the period immediately after the R-wave trigger and during the time required for the application of dummy RF excitations to establish dynamic equilibrium. The left ventricular end-systolic volume also could have been underestimated in some cases because they did not use view sharing.

Although many more intermediate images can be generated by means of variations in the proportion of data shared, we chose to use only half of the data from the original temporally adjacent data sets. This view-sharing scheme allowed us to increase the number of temporal-phase images from m to $2m - 1$ and to improve the effective temporal resolution from $n \times$ TR to $n/2 \times$ TR, in which m is the number of cardiac phases acquired without view sharing. We present data from a mathematic simulation in addition to data from studies that involved patients and volunteers to demonstrate the improvement in the ability to estimate the end-systolic and end-diastolic ventricular volumes with view sharing and uniform TR RF excitation.

THEORY

The view acquisition order used in fast cardiac imaging, unlike that used by Atkinson and Edelman (1), is sequentially segmented rather than interleaved. If the k-space views are labeled from 1 to 128 and n = eight views per segment, views 5–12 are acquired with the first cardiac trigger, followed by views 13–20 on the next trigger, and so forth. The remaining views, 1–4 and 125–128, are acquired after the last cardiac trigger. This k-space traversal pattern was selected to ensure that the low spatial frequency views, 61–68, would be acquired within a single RR interval. This reduces the presence of image artifacts due to trigger-to-trigger variations. In comparison with the interleaved segment view order, images acquired with the sequential segmented order exhibited fewer image artifacts. Because adjacent spatial frequency data are acquired close together in time, images with a sequential segmented order appear to have better edge definition. The choice of a sequential segmented order did not impair image quality or clinical diagnosis, as noted in an earlier study (8), in which the overall quality of fast cardiac images was judged to be superior to that of ECG-gated spin-echo images.

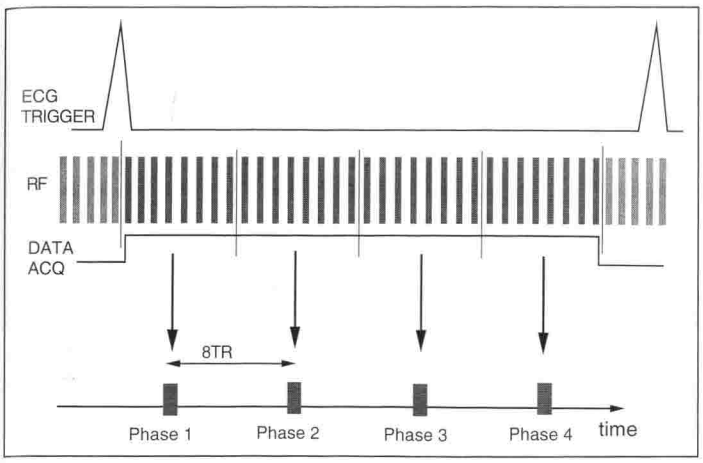

1.

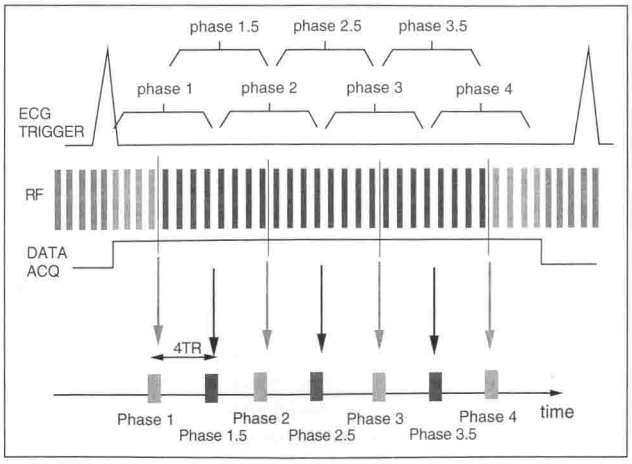

2.

Figures 1, 2. **(1)** Diagram shows the uniform TR RF excitation and prospectively gated data acquisition scheme for a fast cardiac pulse sequence. Eight views are grouped into a segment to generate data for the temporal-phase images (vertical arrows). Note that with uniform TR RF excitation, the steady state is maintained, and the first phase is closer to the R wave, as dummy excitations are absent. **(2)** With view sharing, the data acquisition is unchanged. However, the data from the adjacent temporal phases in **1** are now combined to generate intermediate data sets at time points midway between those of the original temporal phases. This is equivalent to shifting the acquisition window for a segment by four TR intervals. Although the effective temporal resolution is increased to four TR intervals, motion in each image is still averaged for the eight TR periods. Hence, the true temporal resolution remains unchanged. Note that the intermediate images are averaged over temporal periods different from those in **1**.

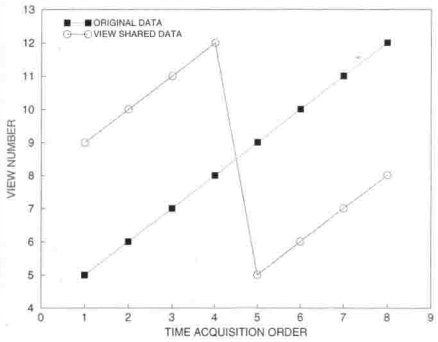

Figure 3. Diagram shows view acquisition order within a segment for a fast cardiac sequence with eight views per segment. In the original temporal-phase images, all views are acquired in sequential order. In the view-shared images, a discontinuity arises in the k-space views within a segment (and within data from the same RR interval). In our study, this discontinuity did not generate additional image artifacts.

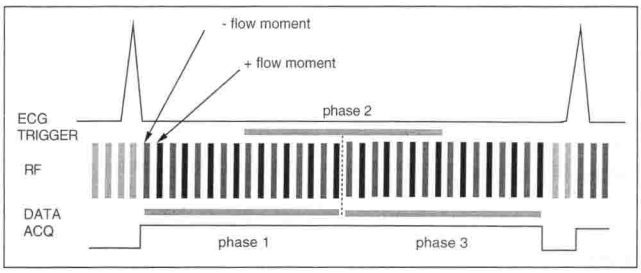

Figure 4. Diagram shows the VENC scheme in a fast cardiac PC acquisition. This example shows flow encoding in a single direction with eight views per segment. Note that with view sharing, three phases can be obtained with twice the temporal resolution of those obtained without view sharing. Note that the plus and minus flow-encoding moments are acquired as sequential pairs.

In a fast cardiac acquisition, the original multiphase images have a temporal resolution of $n \times$ TR, where n is the number of views per segment (Fig 1). Our view-sharing scheme uses the last $n/2$ views in each segment of one temporal-phase image with the first $n/2$ views in each segment of the succeeding temporal phase to generate a data set for the intermediate image. A diagram of this method is shown in Figure 2. In this manner, if m temporal-phase images are originally obtained with fast cardiac imaging, the method described will almost double the number of temporal-phase images to $2m - 1$. Although the temporal-phase images are segmented by shorter intervals, each image is still an average for the time required to acquire data for all n views within a segment such that the true temporal resolution is unchanged. However, the effective temporal resolution is doubled, as the temporal separation between each image is now halved. The data for the intermediate image represent data averaged for the same period but at a time different from that of the original images. Consequently, for an object such as the beating heart, the view-shared image can be considered to be a snapshot of motion at a time midway between that of the original images. View sharing does not alter the image acquisition time or the actual number of data or view acquisitions.

This view-sharing scheme can also be thought of as a shift of a virtual acquisition window by $n/2$ views for the acquired data per RR interval to generate the intermediate data sets. We could have easily shifted this virtual acquisition window by one view, which would have generated an n-fold increase in the number of temporal phases and would have increased the effective temporal resolution to a TR interval. However, this would result in an excessive number of images (>60 images per location, >600 images per series for 10 locations) and would yield only incremental new information. The sharing of $n/2$ views ensures that the intermediate images represent maximal change from the source images and that some economy in data storage is attained.

In the original temporal-phase images, each k-space view is incremented sequentially within a segment. However, in the intermediate images, view sharing introduces a discontinuity in the data acquisition order, as shown in Figure 3. As the discontinuity is in

the middle of an acquisition segment and all views within a segment are acquired in the same RR interval, it was determined that the presence of this discontinuity in the view-shared data set did not compromise image quality. The discontinuity arises at the segment boundaries, and these occur at different spatial frequencies except at the low spatial frequencies about $k_y = 0$, where ky is the k space in the y direction.

To simulate the effects of view sharing, a mathematic model of an anulus was constructed. Contraction of the left ventricle, as seen in the short-axis view, was simulated by means of variation of the outer diameter of the anulus from 110 to 80 pixels and variation of the inner diameter from 90 to 40 pixels. This model allowed us to generate different radial velocities for both the epi- and endocardial borders. Because the end-systolic state persists for some time, a dwell time was also specified in our model. This dwell time determined how long the cardiac model was at the minimum inner and outer diameters in end systole.

In our model, we assumed a heart rate of 72 beats per minute and a sequence TR of 10 msec for an RR interval time of 830 msec divided into 83 time points. In one simulation, the end-systolic point (defined in time-point units) was designated to occur at $t = 31$. In another simulation, $t = 35$ was the end-systolic point. In the former case, this definition ensured that end systole occurred at the temporal boundary between the images without view sharing; in the latter case, it ensured that the point of minimum ventricular area occurred in the middle of an acquisition segment in a non–view-shared image. The dwell time at minimum area in both cases was two time points (20 msec). In the case of $t_{systole} = 31$, we expected that minimum ventricular area would be measured in the view-shared image.

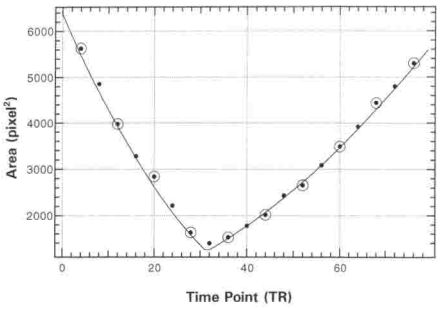

5.

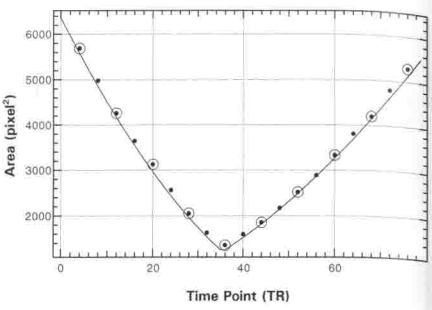

6.

Figures 5, 6. **(5)** Plots of measured ventricular area as a function of time in a cardiac model. • = view-shared data points, ⊙ = original data points, solid line = expected area plotted as a function of time. Note that when the end-systolic state occurred at the temporal boundary between the original images at $t = 31$, the view-shared image provided a better estimation of the end-systolic ventricular area. **(6)** Plot of measured ventricular area as a function of time in a cardiac model for an end-systolic state that occurs at $t = 35$. For the end-systolic state that occurs in the middle of an acquisition segment, the end-systolic ventricular area is correctly depicted in a non–view-shared image.

MATERIALS AND METHODS

The pulse sequence used was a fast gradient-recalled echo sequence with RF phase spoiling. In fast cardiac imaging, RF excitation pulses were applied uniformly throughout imaging, even during the trigger-window dead time when no data were being collected. This maintains the spins in a steady state and obviates dummy excitations before data collection. The use of a uniform TR RF excitation throughout the acquisition allows data collection to be started immediately after the detection of the ECG R-wave trigger. The reason for acquiring the first temporal-phase image immediately after the R wave was to try to provide a better assessment of the end-diastolic state.

Uniform TR RF excitation was used throughout imaging even though the data acquisition was prospectively gated (Fig 1). After each TR sequence, the image-control software polls the signal-processing board in the MR imager to determine whether a valid ECG trigger has been received. The TR sequence is repeated (with data acquisition disabled) until a valid trigger is received, after which time data acquisition commences. Use of uniform TR RF excitation helps avoid artifacts that are caused by an interruption of the steady state; these artifacts were encountered in the earlier breath-hold cardiac studies (1). In addition, maintenance of the steady state helps to avoid the increased signal intensity in the first few temporal-phase images that is caused by the longer T1 recovery period; the so-called lightning-flash artifact is avoided. An additional advantage of beginning data acquisition immediately after detection of the ECG trigger is that the first temporal-phase image is acquired closer to the R wave, and so better visualization of the end-diastolic state is provided.

All MR images were obtained with a 1.5-T system (GE Medical Systems).The volunteer studies were performed with ECG gating and a prototype phased-array coil (9,10) specifically designed for pulmonary-cardiac experiments. The head transmit-receive coil, the body transmit-receive coil, or the receive-only phased-array coil was used in adults and children, depending on coil availability. Breath holding, when tolerated by patients, was used in the adult studies. In the other studies, including those that involved children, a non–breath-hold, four-excitation protocol was used. The ventricular areas were measured on the resulting images by means of manual tracing of the myocardial–blood pool boundaries. These areas were then plotted as a function of cardiac delay time.

A timing diagram of the fast cardiac PC pulse sequence is shown in Figure 4. For each k-space view, two or four flow-encoding sequences were acquired, depending on whether the acquisition was sensitive to a single direction or to all three flow directions (11). The gradient waveforms produced two-sided flow encoding (12); that is, the first gradient moment was toggled symmetrically about zero. To quantify flow in a single direction, the number of required views is twice that in a fast cardiac acquisition. Thus, the total number of views required for PC acquisition is $(n_{flow} + 1) \times yres$, in which $n_{flow} = 1$ or 3 is the number of flow directions chosen, and *yres* is the matrix dimension in the phase-encoding direction. The effective temporal resolution of a fast cardiac PC acquisition is thus $n \times (n_{flow} + 1) \times TR$ without view sharing and $[n \times (n_{flow} + 1) \times TR]/2$ with view sharing in which 50% of the views from adjacent temporal segments are used. Both healthy volunteers and patients underwent imaging with fast cardiac PC.

To verify the accuracy of the velocity flow measurements of fast cardiac PC, a constant-flow phantom was imaged with both fast cardiac PC and conventional cine PC sequences with a range of flow rates (400–1,600 mL/min). The flow measurements obtained with the two techniques were then compared. The flow measurements were also compared with those obtained with an FM2000C digital flow meter (Stellar Instruments, Irvine, Calif), which was used to verify the actual flow rate. The effective temporal resolution attained with fast cardiac PC can be as short as 12–15 msec with view sharing; similar temporal resolution can be attained with conventional cine PC only by means of linear interpolation. Flow measurements were also compared in healthy volunteers.

For the mathematic simulations, a two-dimensional fast Fourier transformation was performed in the annular cardiac model at each time point. As the cardiac model varied in a function of time, the k-space data for each time point were generated. The appropriate k-space views for each time point were then stored in sepa-

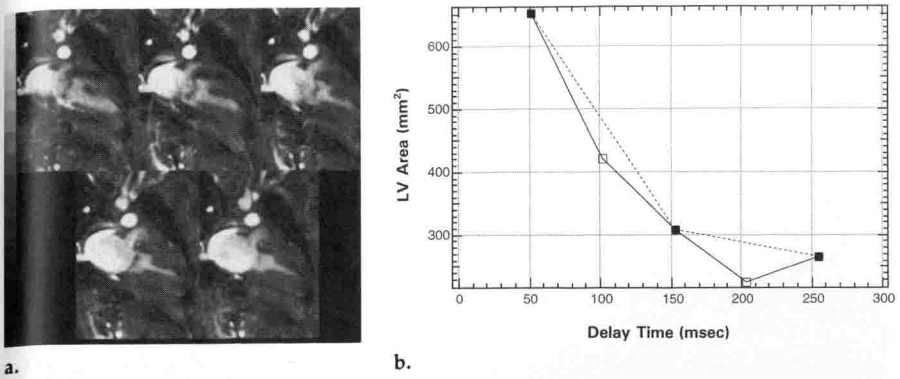

a. b.

Figure 7. **(a)** Oblique coronal images (12.8/5.4 [TR msec/echo time msec]) in a 19-month-old male patient. Because of the high heart rate (154 beats per minute), only three phases were obtained without view sharing. View sharing increased the number of phases to five and allowed a more accurate measurement of the end-systolic left ventricular area. The temporal resolution of these images after view sharing was 51 msec. Acquisition parameters consisted of a field of view of 24 cm, a matrix of 256 × 128, a section thickness of 5 mm, a flip angle of 30°, and four signals acquired. In this examination, the patient was sedated and a head coil was used. **(b)** Plot shows the left ventricular area and delay time. Dashed lines = values obtained when view sharing was not used, □ = view-shared data points, ■ = non–view-shared data points (original acquisition).

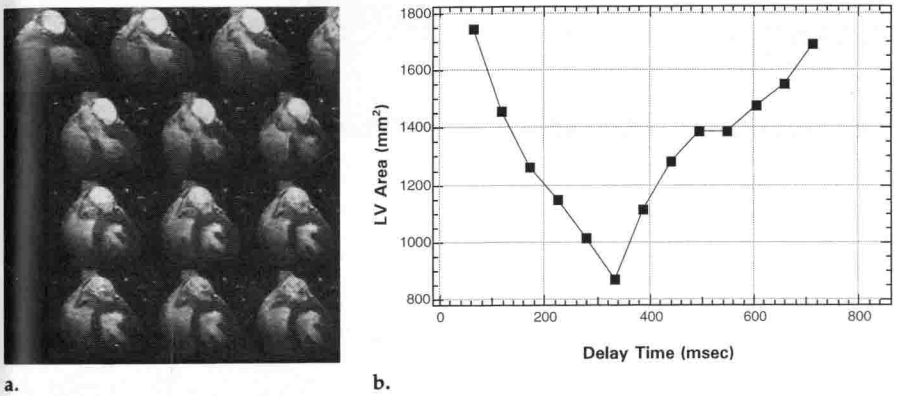

a. b.

Figure 8. **(a)** View-shared coronal images (12.9/4.9) were obtained with a phased-array coil in a healthy 27-year-old male volunteer (heart rate, 81 beats per minute). The temporal resolution of these images after view sharing was 51 msec. Acquisition parameters consisted of a field of view of 28 cm, a matrix of 256 × 128, a section thickness of 5 mm, and a flip angle of 30°. The images were obtained during a single breath hold. Good contrast between the myocardium and the blood pool was demonstrated in all images. Note the variation in left ventricular chamber size in the different temporal-phase images. **(b)** Measured left ventricular area and delay time are plotted from the images. Every other data point beginning with the second measurement was from a view-shared image. In this study, the minimum systolic volume was determined from a view-shared image. With view sharing, the error in the measurement of systolic left ventricular volume was minimized.

rate data files that corresponded to the temporal-phase images. In these simulations, as in the patient and volunteer experiments, eight views per segment were used. View sharing of k-space data from the original images was used to generate the intermediate-image data sets. The data were then filtered by means of a radially dependent apodizing window before the use of an inverse two-dimensional fast Fourier transformation to reconstruct the images.

The ventricular area was measured for each temporal phase with the region-of-interest tool at an Advantage Windows workstation (GE Medical Systems) and plotted. For consistency, the ventricular edges were defined as the point of half maximum image signal intensity. The measured data samples were then compared with the expected ventricular area. The time of each segment was defined as the middle of the segment acquisition period.

RESULTS

The results of the simulation are shown in Figures 5 and 6. In both cases, the measured ventricular areas correlated closely with the predicted values. As expected, when the end-systolic state occurred at the temporal boundary between adjacent temporal segments (Fig 5), the measurements in the non–view-shared images overestimated the end-systolic area. The view-shared image provided a more correct representation of the end-systolic ventricular area. However, if the time at which the area was at its minimum was in the middle of an acquisition segment (Fig 6), then no additional information was gained from the view-shared image. Nevertheless, the additional view-shared images allowed a smoother depiction of the ventricular motion when the images were displayed in a cine loop.

In the simulations, the EF in Figure 5 was calculated as 75.2%. The true EF of the simulated heart was 80.2% when 40 and 90 were used as the end-systolic and end-diastolic radii, respectively. When the view-shared data were not included, the EF was 72.8%. When neither view sharing nor uniform TR RF excitation were considered, the EF was 71.1%. These results suggest that the methods proposed minimize underestimation of ventricular volumes from fast cardiac imaging data.

Figure 7 shows a view-shared sequence of images in a 19-month-old infant with congenital heart disease. At a heart rate of 154 beats per minute, data for only three temporal phases could be acquired with an effective temporal resolution of 102 msec per image with n equal to eight views per segment. More phases could be obtained when the number of views per segment was reduced. In such acquisitions in which breath holds were not required, fewer views per segment could be used without image quality being compromised. When view sharing was used, the number of temporal phases was increased to five, although image acquisition time was constant. The effective temporal resolution was increased to 51 msec per image. When the ventricular areas were plotted as a function of time (Fig 7b), the minimum end-systolic area was measured in a view-shared image. The ventricular EF in this case was 65.5% when all images were considered and 59.4% when the view-shared images were omitted. When we assumed that nonuniform TR RF excitation was not used, the EF was 14.0%. This error is extraordinarily large because only two phases could be acquired with nonuniform TR. In clinical practice, an EF would not be calculated if there were so few data points for a patient.

Figure 7b demonstrates that the ventricular area measured in the view-shared images was not a simple average of the non–view-shared areas but was a representation of the cardiac state at that intermediate time. This finding is consistent with the hy-

pothesis that the view-shared images are the equivalent of a shift of the segment acquisition period by $n/2 \times TR$ rather than a linear interpolation of the original temporal-phase data.

In Figure 8, 13 phases from a view-shared breath-hold acquisition in a healthy volunteer are shown. The corresponding measurement of the left ventricular area is shown in Figure 8b. In this example, the end-systolic state again occurred in a view-shared image. The measured left ventricular EF was 50.2%, compared with 41.9% when the view-shared images were not considered. This finding demonstrates that inadequate temporal resolution may result in a relative error of at least 16% in the measured ventricular EF numbers. View sharing minimizes this error because it restores adequate, effective temporal resolution in fast image acquisition, even when breath-hold techniques are used. In addition, when both view-shared and uniform TR data were excluded, the left ventricular EF was 40.1%.

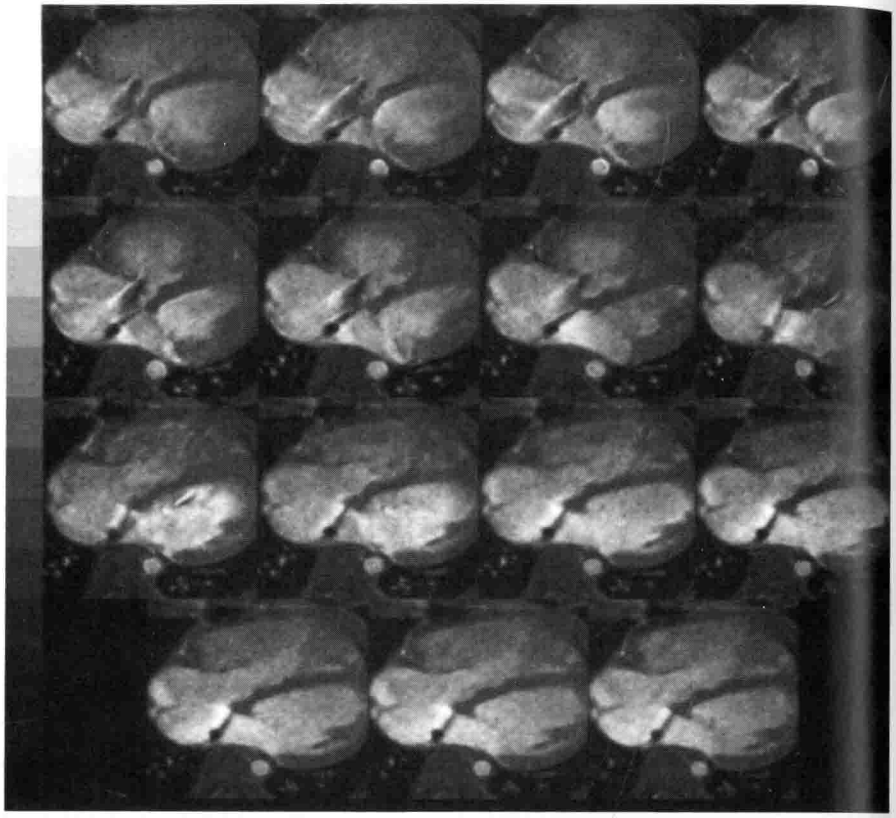

Figure 9. Coronal view-shared images (12.9/4.9) in a 9-year-old patient with tricuspid valve regurgitation (heart rate, 75 beats per minute). Fifteen phases with a temporal resolution of 51 msec were obtained with four signals acquired. Acquisition parameters consisted of a matrix of 256 × 192, a field of view of 32 × 16 cm, a section thickness of 4 mm, and a flip angle of 20°. Note the flow dephasing that results from the jet flow during systole. Adjacent to the region of reduced signal intensity, which is due to flow dephasing, is a region of increased signal intensity. This is due to inflow enhancement that accompanies the regurgitant jet flow. (Images courtesy of Estelle Bank, MD, Department of Radiology, Egelston Children's Hospital, Atlanta, Ga.)

DISCUSSION

Just as view sharing can help improve the accuracy of estimation of the left ventricular end-systolic volume, uniform TR RF excitation is also beneficial in the measurement of left ventricular end-diastolic volume. One can simulate an acquisition without uniform TR by ignoring the first cardiac phase, assuming that a set of dummy acquisitions is necessary to establish dynamic equilibrium. When this is assumed, the left ventricular end-diastolic volume is 3.2% less than the true left ventricular end-diastolic volume, as is the case in Figure 8. To measure accurately the end-diastolic state, data acquisition must begin immediately after the R wave. This is only possible with uniform TR RF excitation. The errors that occur in the measurement of left ventricular end-diastolic volume are far less than those of left ventricular end-systolic volume. Hence, view sharing has a far greater impact on minimization of error in EF measurements.

As shown with the breath-hold technique in Figure 8, good definition of edges was observed; however, a high spatial frequency ghost was observed off the aorta during systole due to pulsatile flow. This distinct ghost was the result of the use of a sequentially segmented rather than an interleaved segmented view acquisition order. Although there was an observable ghost with this view order, there was a definite improvement in edge definition compared with that in the interleaved segmented order. Furthermore, the interleaved segmented order merely smeared out the signal intensity from the ghost over the entire image in the phase-encoded direction.

Figure 9 shows a sequence of 15 phases that demonstrates tricuspid valve regurgitation in a 9-year-old patient. The jet flow that results from the regurgitation during systole is clearly seen as a region of flow dephasing that emanates from the valve. As the valve leaflets open during diastole, the jet-flow phenomenon diminishes. All view-shared fast cardiac images demonstrated high myocardial–blood pool contrast, good edge definition, and a lack of substantial image artifacts. When images with an effective temporal resolution of 40–50 msec (depending on sequence TR) were routinely obtained, the temporal resolution of the fast cardiac sequence almost matched that of conventional cine MR imaging. In addition, between nine and 19 phases of the cardiac cycle (depending on heart rate) could be easily obtained. This example demonstrates that view sharing is effective even in a multiple-excitation study and in a rapidly changing event (in this case the flow phenomena of the regurgitation).

For quantitative flow analysis, we compared measurements of the volume flow rate through flexible plastic tubing (Tygon; Norton Performance Plastics, Akron, Ohio) that had a 1-cm inside diameter; measurements were obtained with both fast cardiac PC and a standard, retrospectively gated PC pulse sequence, cine PC (13). The rate of flow varied between 400 and 1,600 mL/min and was monitored with a digital flow meter. The meter had been previously calibrated by means of the timed filling of a graduated cylinder and had an accuracy of better than ±1% in this flow range. The flow rate measured with fast cardiac PC and averaged for all the cardiac phases had a slope of 1.003 ± 0.013 (standard deviation) with a cor-

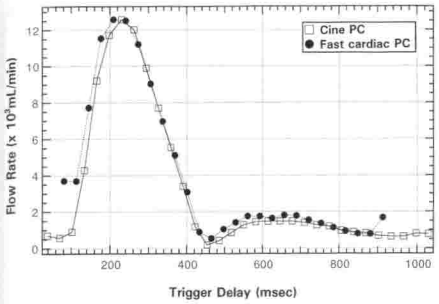

Figure 10. Flow rates were measured with view-shared fast cardiac PC and conventional cine PC in the descending aorta of a healthy volunteer. The VENC was set at 120 cm/sec with flow sensitivity in the cranial-caudal direction. The acquisition parameters for cine PC images (20/8.1) consisted of a flip angle of 30°, a matrix of 256 × 192, a field of view of 32 × 24 cm, and a section thickness of 7 mm. The temporal resolution of this acquisition was 40 msec, which was interpolated to 33.3 msec (32 phases with a heart rate of 58 beats per minute). The acquisition parameters for fast cardiac PC were identical to those of cine PC except that TR was 15.9 msec and echo time was 8.1 msec, and there were two views per segment. Temporal resolution of fast cardiac PC was 63.6 msec with an effective temporal resolution of 31.8 msec after view sharing (27 phases). Note the excellent correlation. Acquisition time was 2.5 minutes for cine PC and 1.3 minutes for fast cardiac PC. Delay times for fast cardiac PC were offset by +40 msec.

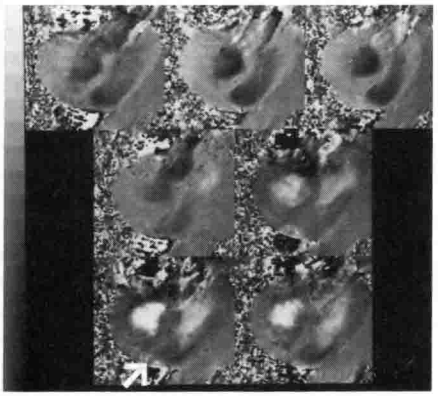

Figure 11. View-shared fast cardiac PC images (21.5/10.7) in a healthy volunteer were obtained with a 21-second breath hold. The oblique, short-axis view shows flow in the left anterior descending branches (arrow). Acquisition parameters consisted of a field of view of 24 × 18 cm, a section thickness of 5.0 mm, a matrix of 256 × 128, one signal acquired, a VENC of 100 cm/sec, and a flip angle of 15°, with four views per segment and a heart rate of 75 beats per minute. A surface coil with a 7.6-cm diameter was also used. (Images courtesy of Hajime Sakuma, MD, Department of Radiology, University of California, San Francisco.)

relation coefficient of .9995 when plotted against the true flow rate. Seven flow-rate values were obtained. The fast cardiac PC measurements were also within a standard deviation of the cine PC measurements. We conclude that fast cardiac PC can be used to quantify instantaneous flow rate with an accuracy similar to that with cine PC.

Figure 10 shows the instantaneous flow rate in the descending aorta measured with both cine PC and fast cardiac PC in a healthy volunteer. There is excellent correlation between both sequences in the flow measurements. The delay times for fast cardiac PC were offset by +40 msec relative to the cine PC delay times. This was performed to account for an instrument-related offset. Fast cardiac PC images were acquired in approximately half the time of a conventional cine PC acquisition: 1 minute 17 seconds versus 2 minutes 31 seconds. The cine PC sequence involves acquisition of data during the entire cardiac cycle, which can be an advantage. We are investigating a modification to the view-sharing technique that eliminates the "blind spot" in both fast cardiac PC and fast cardiac acquisition sequences. Both fast cardiac PC and cine PC images were acquired with a body coil, a 256 × 192 matrix, a three-fourths asymmetric field of view, one signal acquired, and an aliasing VENC value of 120 cm/sec. The fast cardiac PC image used four views per segment and generated 27 phases (with view sharing) for an effective temporal resolution of 32 msec. The data in Figure 10 show that view sharing in a quantitative flow experiment can accurately depict a rapidly changing event, such as changes in signal intensity and phase due to pulsatile flow. This is also clearly demonstrated in breath-hold fast cardiac PC images of the heart, as shown in Figure 11. There is good depiction of flow in the left and right ventricles and in the coronary arteries. It is clear that the use of breath holding in a quantitative flow examination, such as one with fast cardiac PC, eliminates respiratory motion artifacts and improves the accuracy of velocity measurements.

Whereas the effective temporal resolution in cine PC is interpolated, that of fast cardiac PC is not. The true temporal resolution in cine PC is determined from the sequence TR and the number of flow directions selected, which may be in the range of 40–150 msec (depending on image parameters). In extreme cases in which the true temporal resolution of a cine-PC acquisition is 100 msec with an effective (interpolated) temporal resolution of 20 msec, a fast cardiac PC acquisition with the same effective temporal resolution would have greater accuracy. This is because the data are not interpolated.

In conclusion, in the determination of cardiac function, especially in ventricular EFs, an effective temporal resolution of at least 40–50 msec is required. This temporal resolution cannot be attained with fast gradient-echo acquisitions if all imaging is to be completed with conventional gradient subsystems in which a 10- to 15-second breath hold is used. View sharing allows us to attain effective temporal resolution while maintaining a short imaging time so that a breath-hold acquisition is possible. View sharing and uniform TR RF excitation substantially improved our ability to measure the end-systolic and end-diastolic ventricular volumes. In addition, when applied to a fast cardiac PC acquisition, view sharing substantially improved the effective temporal resolution of the quantitative or directional flow study. In both fast cardiac and fast cardiac PC, almost equivalent velocity and flow information was obtained compared with that of conventional cine MR and cine PC MR imaging but with markedly reduced imaging times. The ability to acquire both cine and PC cine MR images within a breath hold and with reasonable temporal resolution affords improvement in image quality because it reduces respiratory artifacts. ■

References

1. Atkinson DJ, Edelman RR. Cineangiography of the heart in a single breath hold with a segmented TurboFLASH sequence. Radiology 1991; 178:357–360.
2. Utz JR, Hefkens RJ, Heinsimer JR, Shimakawa A, Glover GH, Pelc NJ. Valvular regurgitation: dynamic MR imaging. Radiology 1988; 168:91–94.
3. Riederer SJ, Tasciyan T, Farzaneh F, Lee JN, Wright RC, Herfkens RJ. MR fluoroscopy: technical feasibility. Magn Reson Med 1988; 8:1–15.
4. Laub G. Breath-hold cine MR imaging with a shared and reordered gradient echo technique (abstr). In: Proceedings of the Society of Magnetic Resonance in Medicine 1993. Berkeley, Calif: Society of Magnetic Resonance in Medicine, 1993; 478.
5. Foo TKF, Bernstein T, Aisen AM, Hernandez RJ, Collick BD, Pavlik G. High temporal resolution breath-held cine cardiac imaging using view sharing (abstr). In: Proceedings of the Society of Magnetic Resonance in Medicine 1993. Berkeley, Calif: Society of Magnetic Resonance in Medicine, 1993; 1269.
6. Bernstein MA, Foo TKF, Collick BD. Fast cardiac phase contrast: a multi-phase breathhold technique with view sharing (abstr). In: Works in progress supplement to annual meeting program. Berkeley, Calif: Society of Magnetic Resonance in Medicine, 1994; S23.
7. Sakuma H, Fujita N, Foo TKF, et al. Evaluation of left ventricular volume and mass

with breath-hold cine MR imaging. Radiology 1993; 188:377–380.
8. Hernandez RJ, Aisen AM, Foo TKF. Thoracic cardiovascular anomalies in children: evaluation with a fast gradient-recalled-echo sequence with cardiac-triggers segmented acquisition. Radiology 1993; 188: 775–780.
9. Hayes CE, Hattes N, Roemer PB. Volume imaging with MR phased-array. Magn Reson Med 1991; 18:309–319.
10. Foo TKF, MacFall JR, Hayes CE, Sostman HD, Slayman BE. Pulmonary vasculature: single breath-hold MR imaging with phased-array coils. Radiology 1992; 183: 473–477.
11. Pelc NJ, Bernstein MA, Shimakawa A, Glover GH. Encoding strategies for three-direction phase-contrast MR imaging of flow. J Magn Reson Imaging 1991; 1:405–413.
12. Bernstein MA, Shimakawa A, Pelc NJ. Minimizing TE in moment nulled or flow encoded 2D and 3D GRE. J Magn Reson Imaging 1992; 2:583–588.
13. Spritzer CE, Pelc NJ, Lee JN, Evans AJ, Sostman HD, Riederer SJ. Rapid MR imaging of blood flow with a phase-sensitive, limited-flip-angle, gradient recalled pulse sequence: preliminary experience. Radiology 1990; 176:255–262.